Medicine®

OBSERVATIONAL STUDY

OPEN

Frequency-Specific Local Synchronization Changes in Paroxysmal Kinesigenic Dyskinesia

Zhi-Rong Liu, MD, Huan-Huan Miao, MS, Yang Yu, MS, Mei-Ping Ding, MD, and Wei Liao, PhD

Abstract: The neurobiological basis of paroxysmal kinesigenic dyskinesia (PKD) is poorly defined due to the lack of reliable neuroimaging differences that can distinguish PKD with dystonia (PKD-D) from PKD with chorea (PKD-C). Consequently, diagnosis of PKD remains largely based on the clinical phenotype. Understanding the pathophysiology of PKD may facilitate discrimination between PKD-D and PKD-C, potentially contributing to more accurate diagnosis.

We conducted resting-state functional magnetic resonance imaging on patients with PKD-D (n = 22), PKD-C (n = 10), and healthy controls (n = 32). Local synchronization was measured in all 3 groups via regional homogeneity (ReHo) and evaluated using receiver operator characteristic analysis to distinguish between PKD-C and PKD-D.

Cortical-basal ganglia circuitry differed significantly between the 2 groups at a specific frequency. Furthermore, the PKD-D and PKD-C patients were observed to show different spontaneous brain activity in the right precuneus, right putamen, and right angular gyrus at the slow-5 frequency band (0.01–0.027 Hz).

The frequency-specific abnormal local synchronization between the 2 types of PKD offers new insights into the pathophysiology of this disorder to some extent.

(*Medicine* 95(13):e3293)

Abbreviations: AUC = area under curve, PKD = paroxysmal kinesigenic dyskinesia, PKD-C = paroxysmal kinesigenic dyskinesia with chorea, PKD-D = paroxysmal kinesigenic dyskinesia, ReHo = regional homogeneity, ROC = receiver operating characteristic, ROI = regions of interest, RS-fMRI = resting-state functional magnetic resonance imaging.

INTRODUCTION

Paroxysmal kinesigenic dyskinesia (PKD) is a rare movement disorder characterized by brief episodes of abnormal movement that are triggered by sudden voluntary movements.[1,2] Investigation of the neural mechanisms underlying PKD is a difficult task due to its complex clinical manifestations (e.g., chorea and dystonia).[3–5]

Although PRRT2 mutations have been identified as one type of genetic causes of PKD,[6,7] they cannot be used to differentiate PKD patients with dystonia (PKD-D) and chorea (PKD-C).[8] Neuroimaging of PKD-D, PKD-C or a mixture of both types has also failed to completely define specific neural characteristics that allow differentiation between these disorders.[9,10] At present, diagnosis of PKD mainly relies on these clinical characteristics, in the absence of reliable PKD-D- or PKD-C-specific neuromarkers.[11]

Dysfunctional subcortical structures, particularly the thalamus and basal ganglia, underlie the pathophysiology of PKD.[12–16] Voluntary movement is controlled by basal ganglia-thalamocortical circuits and disruption of these circuits may cause dyskinesia in PKD. Resting-state functional magnetic resonance imaging (RS-fMRI) studies have revealed increased intrinsic activity in the bilateral putamen and cortical-basal ganglia circuitry in PKD patients.[9,10] More recently, increased resting-state interhemispheric functional connectivity in the basal ganglia-thalamo-cortical circuitry has been demonstrated in PKD patients,[17] suggesting that PKD can be considered a circuit disorder and not restricted to localized structural or functional abnormalities.[18,19] Regional homogeneity (ReHo) is an effective measure of local connectivity, which quantifies the functional communication between a center voxel and its neighbors in 3 dimensions.[20] This local synchronization is neurobiologically relevant and dependent upon a combination of anatomical, developmental, and neurocognitive factors.[21] An issue that remains unclear is whether the pathophysiology of PKD is related to abnormal local synchronization in the regions involved in cortical-basal ganglia circuitry.

The use of neuroimaging technique to distinguish between PKD-D and PKD-C could provide insights into the pathophysiology of this disorder. The rationale for combining clinical phenomenology and biological mechanisms is to aid in the clinical recognition of dystonia syndromes.[11] To this end, we analyzed resting-state local functional connectivity to determine the neural basis of PKD-D and PKD-C. The converging and diverging patterns of cortical-basal ganglia circuitry between PKD patients and control individuals were mapped. Predictive models were used to evaluate the diagnostic potential of abnormal neuroimaging,[22] based on the theory that changes

Editor: Bernhard Schaller.
Received: August 23, 2015; revised: February 18, 2016; accepted: March 14, 2016.
From the Department of Neurology (Z-RL, M-PD), the Second Affiliated Hospital of Medial College, Zhejiang University, Hangzhou, China; Center for Cognition and Brain Disorders and the Affiliated Hospital (H-HM, YY, WL), Hangzhou Normal University, Hangzhou, China; Zhejiang Key Laboratory for Research in Assessment of Cognitive Impairments (H-HM, YY, WL), Hangzhou, China; Mental Health Education and Counseling Center (YY), Zhejiang University, Hangzhou, China; and Center for Information in BioMedicine (WL), Key Laboratory for Neuroinformation of Ministry of Education, School of Life Science and Technology, University of Electronic Science and Technology of China, Chengdu, China.

Correspondence: Wei Liao, Center for Information in BioMedicine, Key Laboratory for Neuroinformation of Ministry of Education, School of Life Science and Technology, University of Electronic Science and Technology of China, Chengdu, China
(e-mail: weiliao.wl@gmail.com).
Financial disclosure: all the authors have no financial relationships relevant to this article to disclose.

Funding source: this work was supported by Natural Science Foundation of China (grants no.: 81201155 and 81471653 to W.L.), and China Postdoctoral Science Foundation (grant 2013M532229 to W.L.)

Z-RL and H-HM contributed equally to this study.

The authors have no conflicts of interest to disclose.

ISSN: 0025-7974
DOI: 10.1097/MD.0000000000003293

in local functional connectivity may allow effective discrimination between PKD-D and PKD-C at the individual level.

MATERIALS AND METHODS

Subjects

Thirty-two right-handed patients were diagnosed with idiopathic PKD at the Affiliated Hospital of Zhejiang University School of Medicine, China. PKD was diagnosed according to the following established diagnostic criteria:[2] (1) an identified kinesigenic trigger for the attacks; (2) attacks of short duration (< 1 min); (3) no loss of consciousness or pain during the attacks; (4) control with antiepileptic drugs; and (5) exclusion of other organic diseases. All patients underwent routine MRI and EEG or long-term video-EEG monitoring. To exclude secondary cases, ceruloplasmin, thyroid hormone and parathyroid hormone were examined. Exclusion criteria were: (i) claustrophobia or MRI incompatibility; (ii) presence of focal brain lesions identified using routine MRI; (iii) history of alcohol/drug abuse, neurological or psychiatric diseases or serious physical disease; and (iv) falling asleep during scanning. The following clinical features were obtained: age of onset, disease duration, family history of PKD, history of infantile convulsion, dominantly affected side and body parts, attack frequency, sensory aura and response to antiepileptic drug. We did not provoke dyskinesia in drug-naive patients. After detailed history talking, including medication history and careful physical examination, patients with dyskinesia due to other causes were excluded. The subtypes of PKD (i.e., PKD-D and PDK-C) were evaluated based on the phenomenology of the attacks independently by 2 neurologists (ZL and MD).[23] The 2 neurologists reached agreements on their diagnoses of PKD-D and PKD-C for each patient after discussion. Patients were grouped based on type of PKD (PKD-D, n = 22, 6 females, age [mean ± standard deviation (SD)]: 20.50 ± 6.33 years; PKD-C, n = 10, 5 females, age [mean ± SD]: 18.50 ± 5.60 years) (Table 1). Brief attacks of involuntary movements were triggered by sudden voluntary movement in all patients. All the patients took ceruloplasmin, thyroid, and parathyroid tests.

Thirty-two sex- and age-matched right-handed normal controls (n = 32, 14 females, age [mean ± SD]: 20.00 ± 5.91 years) with no history of neurological disorders, psychiatric illnesses, or abnormalities on MRI examinations were included. Written informed consent was obtained from all the participants. The study was approved by the Local Medical Ethics Committee of the Center for Cognition and Brain Disorders at Hangzhou Normal University, China.

Data Acquisition

Imaging was performed on a 3.0 T MRI scanner (GE Discovery 750) at the Center for Cognition and Brain Disorders at Hangzhou Normal University. Foam padding was used to

TABLE 1. Demographic and Clinical Data

Characteristics	PKD-C (n = 10)	PKD-D (n = 22)	NC (n = 32)	*P* Value
Age (y)	18.50 ± 5.60	20.50 ± 6.33	20.00 ± 5.91	0.68*
Sex (male: female)	5:5	16:6	18:14	0.36†
Handedness (left: right)	0:10	0:22	0:32	—
Education (years)	11.20 ± 3.12	11.85 ± 2.60	13.84 ± 4.36	0.06*
Mean FD (mm)	0.05 ± 0.03	0.04 ± 0.02	0.05 ± 0.02	0.95†
Ceruloplasmin (mg/L)	276.30 ± 65.09	295.4 ± 58.60	—	0.46‡
Thyroid hormones				
TT3 (nmol/L)	1.34 ± 0.20	1.38 ± 0.25	—	0.63‡
FT3 (pmol/L)	3.87 ± 0.52	3.50 ± 0.72	—	0.16‡
TT4 (nmol/L)	71.00 ± 9.10	76.76 ± 7.77	—	0.08‡
FT4 (pmol/L)	11.72 ± 1.47	12.63 ± 1.24	—	0.08‡
Parathyroid hormones (pg/mL)	31.60 ± 8.24	34.07 ± 7.58	—	0.46‡
Age at onset (years)	10.70 ± 1.70	11.23 ± 3.11	—	0.21§
Duration (years)	7.80 ± 6.49	9.32 ± 8.20	—	0.74§
Family history (+:−)	1:9	5:17	—	0.64§
Aura (Y: N)	(4:6)	(11:11)	—	
Attack frequency (<10/d: 10-hundreds/d)	(6:4)	(10:10)	—	
Affected side (L: R: Bil: Alt)	(1:2:5:2)	(5:5:10:2)	—	
Distribution (Arm: Leg: Trunk: Face)	(8:9:0:2)	(19:18:0:7)	—	
Treatment: Naive	0	6	—	
Medication (OXC: CBZ: PHT)	(6:4:0)	(12:3:1)	—	
Prognosis after medication	GOOD:10	GOOD:16	—	

CBZ = carbamazepine, FD = framewise displacement, NC = normal controls, OXC = oxcarbazepine, PHT = phenytoin, PKD-C = paroxysmal kinesigenic dyskinesia experience choreoathetosis, PKD-D = paroxysmal kinesigenic dyskinesia experience dystonia.

Values are mean ± SD.

*One-way ANOVA.

†Kruskal–Wallis ANOVA.

‡Two-sample *t* test.

§Mann Whitney *U* test.

minimize head motion. Subjects were instructed to rest with their eyes closed, not to think of anything in particular and not to fall asleep during scanning. Functional images were acquired using an echo-planar imaging sequence (repetition time/echo time = 2000 ms/30 ms and flip angle = 90°). Forty-three transverse slices (field of view = 220 × 220 mm^2, matrix = 64 × 64, slice thickness = 3.2 mm, no inter-slice gap) were acquired along the anterior–posterior commissure. For each subject, 240 volumes were collected requiring a total scan time of 480 s. 3D T1-weighted anatomical images were acquired in the sagittal orientation using a magnetization-prepared rapid acquisition gradient-echo sequence (repetition time/echo time = 8.06 ms/3.136 ms, flip angle = 8°, field of view = 256 × 256 mm^2, matrix = 256 × 256, slice thickness = 1 mm, no inter-slice gap and 176 slices). After scanning, subjects were asked whether they had fallen asleep during the scan.

Data Preprocessing

Images were preprocessed using DPARSF (V2.3, http://www.restfmri.net).[24] The first 10 functional images per subject were excluded to equilibrate the signal. Subsequent images were corrected with slice-timing and alignment. Individual 3D T1-weighted anatomical images were co-registered as functional images and subsequently segmented into gray matter, white matter, and cerebrospinal fluid. Nonlinear spatial deformation was calculated from the gray matter images to Montreal Neurological Institute space using 12 parameters of an affine linear transformation. Transformation parameters were applied to functional images. Normalized data were resliced at a resolution of 3 × 3 × 3 mm^3. Several sources of spurious variance (head motion parameters derived by Volterra expansion, global brain signal, and average signal calculated from white matter signal and cerebrospinal fluid) were removed using multiple linear regression analysis. After linear detrending, functional images were filtered using the slow-5 band (0.01–0.027 Hz) and slow-4 band (0.027–0.073 Hz).[25]

Regional Homogeneity Analysis

ReHo was calculated by comparing Kendall's coefficient of concordance of the time series of a given voxel with those of its nearest neighbors (27 voxels). Two types of ReHo maps (band range: 0.01–0.027 Hz, 0.027–0.073 Hz) were generated according to previous RS-fMRI studies.[26,27] Individual ReHo maps were normalized to the mean ReHo value of the whole brain. Finally, all ReHo maps were spatially smoothed with a 6-mm full width at a half maximum Gaussian kernel.

Statistical Analysis

Demographic differences between the PKD-D, PKD-C, and control groups were analyzed using 1-way analysis of variance (ANOVA). To investigate the differences in local functional connectivity between the groups, 2-way mixed design ANOVA was performed on each individual standardized ReHo map using GLM_Flex2 (http://mrtools.mgh.harvard.edu/index.php/GLM_Flex). A threshold of $P < 0.05$ was set for the main effect and interaction effect (combined height threshold $P < 0.02$ and cluster size of 48 voxels) using the AlphaSim program, which applied Monte Carlo simulation. Next, we extracted signals from the regions of interest (ROI) showing significantly different interaction effects. Statistical significance between groups was determined using the post-hoc 2-sample t-test ($P < 0.05$, Bonferroni correction).

Correlation Between local Synchronization and Clinical Variables

To investigate the clinical relevance of altered local frequency-specific synchronization in PKD patients, clinical variables (disease duration and age of onset) were separately correlated with ReHo values of ROIs using Pearson correlation analysis in PKD-D and PKD-C groups.

Receiver Operating Characteristic Curves

Receiver operating characteristic (ROC) curves were used to determine the suitability of local functional connectivity as potential neuroimaging differences between PKD-D and PKD-C phenotypes.[28] This ROC analysis was performed at different frequency bands using ReHo values from each ROI. The original area under curves (AUC) of ROC was calculated between the 2 patient groups (PKD-D and PKD-C).

To test statistical significance of the AUC, we used a nonparametric permutation test. In particular, the group labels (PKD-D and PKD-C) were randomly permuted for 1000 times. We then calculated the AUC for each permutation. The P value was defined as the ratio of the frequency of permutations that achieve greater AUC than the original AUC to the total permutation times.[29]

RESULTS

Clinical and Demographic Data

No PKD attacks were reported by patients during the MRI scan. Translation or rotation parameters did not exceed ± 3 mm or ± 3°, respectively. Moreover, mean frame-wise displacement[30] computed for each subject did not differ among the 3 groups ($F = 0.23$, $P = 0.79$). We observed no significant differences in gender, age, or educational levels among the groups. In addition, ceruloplasmin, thyroid, and parathyroid hormones levels of patients with PKD were normal and did not differ between the PKD-C and PKD-D groups (Table 1). Moreover, age of onset and duration did not differ between the PKD-C and PKD-D groups (Table 1). All patients had paroxysmal, brief (usually <1 min) attacks of dystonia (22 patients) and chorea (10 patients), which was exclusively precipitated by sudden voluntary movements. PKD-C patients predominantly manifested rhythmic and oscillatory movement of body parts, whereas PKD-D patients were mainly characterized by sustained muscular contractions. Attacks commonly involved the arms, legs, face, or a mixture (Table 1).

Differences in Regional Homogeneity

Significant differences in ReHo were identified in the right precuneus, right inferior frontal gyrus (opercular part), right putamen, left supramarginal gyrus, left middle frontal gyrus, and left superior temporal gyrus ($P < 0.05$, AlphaSim corrected) (Figure 1 and Table 2). Differences in the right precuneus, right putamen, right angular gyrus, and left superior frontal gyrus between groups were dependent on a specific frequency ($P < 0.05$, AlphaSim corrected) (Figure 2 and Table 2).

We performed a post-hoc 2-sample t-test analysis, to determine the differences between the 3 groups at different frequency bands. At the slow-5 frequency, we observed significant differences between PKD-C and PKD-D in the right putamen ($P = 0.002$), angular gyrus ($P = 0.0005$), and precuneus ($P = 0.0017$) (all $P < 0.05$, Bonferroni corrected) (Figure 2). In addition, significant differences were observed

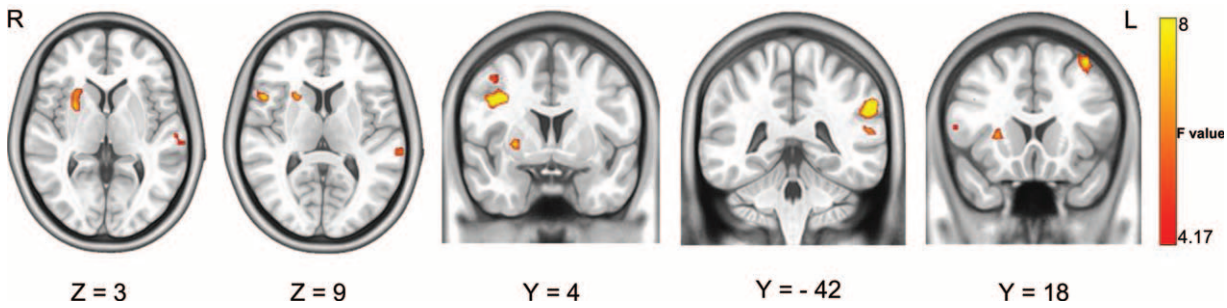

FIGURE 1. ReHo differences among groups, determined using 2-way mixed-design ANOVA. Significant differences in ReHo were observed among the groups in the right putamen, right inferior frontal gyrus (opercular part), left superior temporal gyrus, right precuneus, left supramarginal gyrus, and middle frontal gyrus. ANOVA = analysis of variance; ReHo = regional homogeneity.

between PKD-C patients and controls in the right putamen ($P = 0.0009$) at the slow-5 band (0.01–0.027 Hz). No significant differences were evident among the groups at the slow-4 band (0.027–0.073 Hz).

Local synchronization was not significantly affected by disease duration or age of onset.

ROC Analysis

ROC analyses confirmed that PKD-D and PKD-C phenotypes can be effectively distinguished by local functional connectivity at the slow-5 band (0.01–0.027 Hz) for all ROIs (averaged AUC of 81.03) (Figure 3). AUCs were significantly higher than those expected by chance (all $P < 0.05$, permutation test). Optimal performance was achieved in the right angular gyrus at the slow-5 frequency, with an accuracy of 85.91%, sensitivity of 81.8%, specificity of 80.0%, and AUC of 0.8591. ROC curves between PKD-C and PKD-D were distinguished using ReHo values (Figure 3). The performance of ROC at the slow-4 band (0.027–0.073 Hz) was less accurate than that at the slow-5 band.

TABLE 2. Brain Regions With Differences in ReHo Between the PKD-C, PKD-D, and Control Groups

Brain Region	BA	MNI Coordinates (*x y z*) (mm)	Voxels	ANOVA (*F* Value)
ReHo at group main effect				
Right PCUN	6, 9	(36,3,33)	67	11.49
Left SMG	40	(−60, −42, 33)	72	10.43
Right IFGoperc	44	(51, 15, 9)	67	8.67
Right PUT	N/A	(27, 6, 0)	54	8.50
Left MFG	6, 8	(−39, 18, 57)	55	8.31
Left STG	21, 22	(−57, −42, 15)	67	6.97
ReHo at interaction effect				
Left SFG	8, 9	(−18, 54, 42)	68	10.33
Right PCNU	7	(9, −75, 57)	103	9.77
Right PUT	N/A	(21, 6, 6)	57	8.98
Right AG	19, 39	(39, −75, 39)	72	7.91

x, *y*, *z*, coordinates of primary peak locations in the MNI space.

AG = angular gyrus, BA = Brodmann area, IFGoperc = inferior frontal gyrus (opercular part), MFG = middle frontal gyrus, MNI = Montreal Neurological Institute, N/A = not applicable, PCUN = precuneus, PUT = putamen, SFG = superior frontal gyrus, SMG = supramarginalgyrus, STG = superior temporal gyrus.

DISCUSSION

Analysis of functional neuroimaging in patients with PKD has failed to define the distinct neural characteristics of PKD-D and PKD-C.[9,10,13,15,17,31] Consequently, diagnosis remains based on clinical symptoms that are diverse and vary between individuals.[5] To this end, we investigated the distinct neural characteristics of PKD-D and PKD-C.

PKD is characterized by short episodes of involuntary movement attacks triggered by sudden voluntary movements.[2] However, limited movement-related fMRI studies to date have focused on involuntary movements. Recently, Onofrj et al observed that levitation and tentacular movement-related involuntary movements induce brain activity.[32] The isolated brain activation of contralateral primary motor cortex suggested that levitation and tentacular movement-related involuntary movements are cortical disinhibition symptoms.[32] Resting-state fMRI (in the absence of movement) presented evidence of hyperconnectivity in the PKD and provided theoretical explanations for movement-related fMRI findings.[17]

We investigated the brain frequency-specific (0.01–0.027 Hz and 0.027–0.073 Hz) local synchronization of PKD-D and PKD-C via ReHo analysis. However, no local synchronization differences were evident between PKD-D and controls, distinct from previous resting-state fMRI findings.[10] Earlier, Zhou et al observed abnormalities in the amplitudes of low frequency fluctuations (0.01–0.08 Hz) between mixed PKD-D and PKD-C group and controls.[10] It is possible that not only distinct resting-state measurements but also the frequencies selected partially account for these differences. Importantly, the effects of anti-epileptic drugs on the results cannot be overlooked.[33] Although all patients from both studies displayed good outcomes (Table 1), the effects of these drugs on the disorder remain unclear and may contribute to the inconsistent findings. Analysis of differences between drug-naive patients and controls would therefore be of significant interest.

We observed significant alterations in the right precuneus, right putamen, and right angular gyrus in PKD-D and PKD-C patients, suggestive of abnormal spontaneous brain activity, which was specific to the slow-5 frequency band. These differences in ReHo may represent neuromarkers for PKD-D and PKD-C phenotypes at an individual level and thus contribute toward a deeper understanding of the pathological mechanism of the disease.

The putamen is an integral part of the motor circuit.[34,35] We observed spontaneous brain hyperactivity in the putamen of

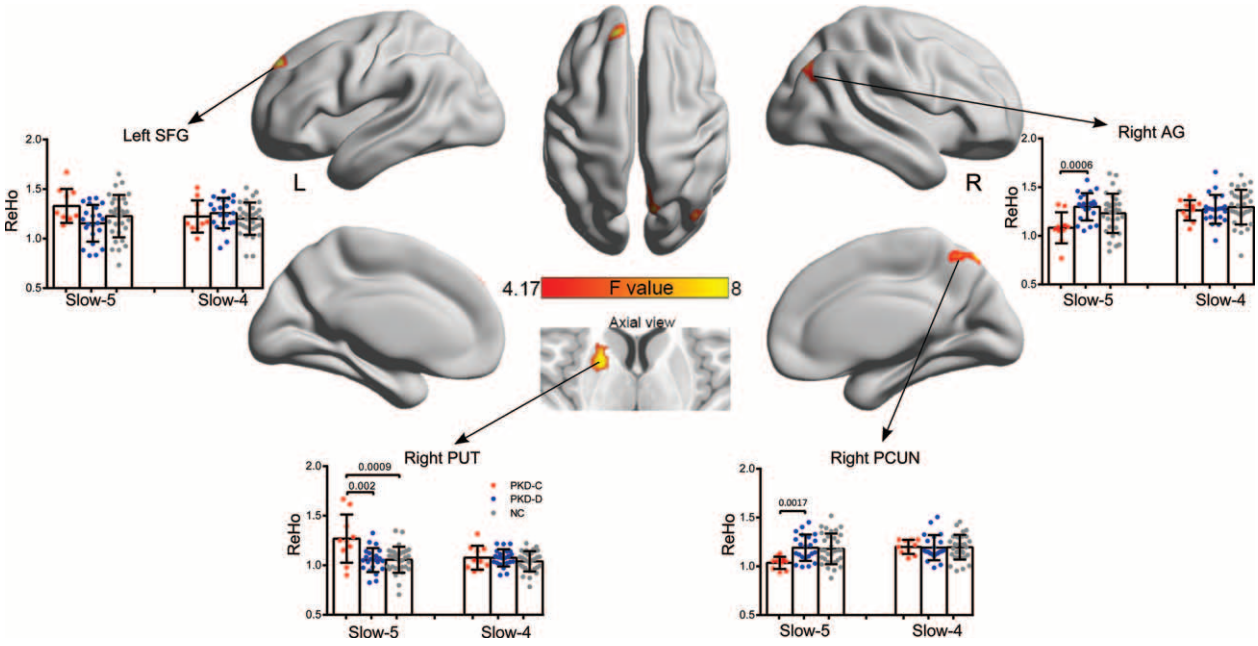

FIGURE 2. Interaction effects between frequency bands and groups on ReHo examined using 2-way mixed design ANOVA and post-hoc tests. Significant differences in ReHo identified based on the interaction effects were observed in the right precuneus, right putamen, right angular, and left superior gyrus. $P < 0.05$, Bonferroni correction for number of ROI and times for comparison. ANOVA = analysis of variance; ReHo = regional homogeneity.

PKD patients, in agreement with previous findings.[9,10] Significant atrophy has been reported in the putamen and caudate of individuals with chorea (Huntington's disease)[36,37] and increased activation in the putamen of patients with dystonia.[38] Our current findings and previous reports collectively implicate the putamen in a basal ganglia-thalamic circuit in the pathogenesis of idiopathic PKD-C.

We additionally observed increased spontaneous brain local synchronization in the precuneus of PKD patients for the first time. The precuneus is thought to denote a sensorimotor processing area in both monkeys and humans.[39,40] Therefore, disruption of the precuneus may also contribute to the mechanism of idiopathic PKC. Although significant differences in brain regions among the 3 groups were observed, the intensity

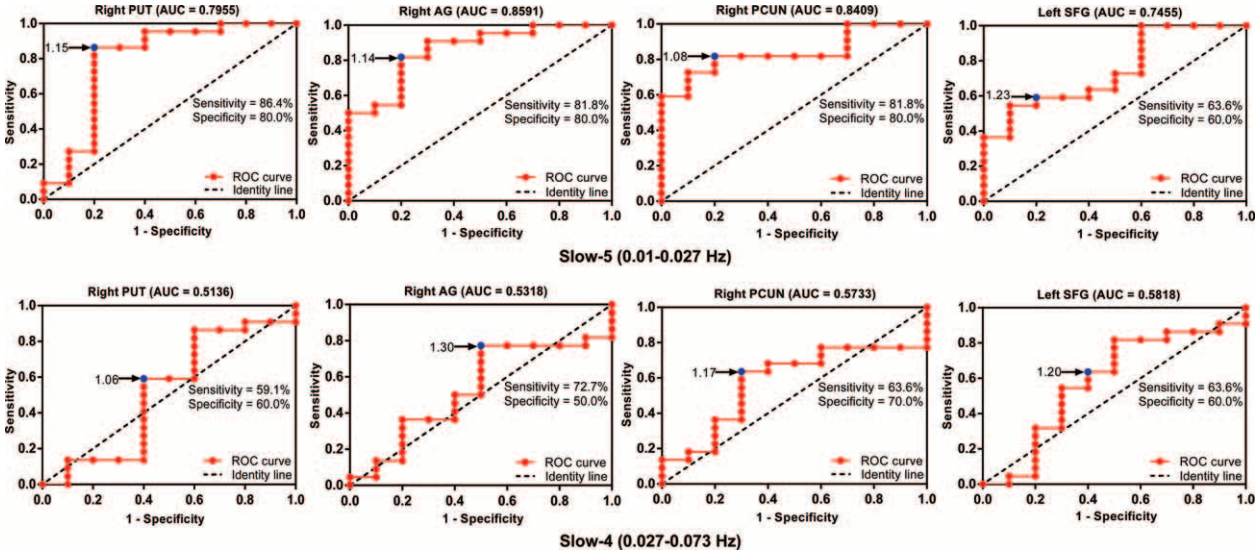

FIGURE 3. ROC curves for discrimination between PKD-C and PKD-D in each ROI at different frequency bands. Blue dots represent cut-off values. AUC = area under curve; PKD-C = paroxysmal kinesigenic dyskinesia with chorea; PKD-D = paroxysmal kinesigenic dyskinesia; ROC = receiver operating characteristic; ROI = regions of interest.

of local synchronization varied across these regions, with discrepancies between PKD-C and PKD-D patients. PKD-C patients showed a greater intensity of local synchronization in right putamen than PKD-D, but lower intensity in the right precuneus and angular gyrus, implying that the pathogenic mechanisms underlying the different clinical phenotypes are complex. Detailed and comprehensive investigations are therefore required to establish the pathology of the disorder.[9,10,17]

Our data showed remarkable asymmetry, in contrast to previous results.[10,12] Earlier structural[12,15] and functional[10,17] studies suggested bilateral abnormality in cortical-basal ganglia-thalamus circuitry regions, including thalamus and putamen, a common pathophysiology in PKD. From the relatively detailed clinical information, we concluded that attacks were predominantly left-sided in 12 patients, including unilateral, bilateral, and alternating cases, and right-sided in 10 patients. Although the difference in number between left- and right-sided patients was small, the asymmetric trend cannot be overlooked. Moreover, diagnosis of the affected sides mainly relied on the history and reports of patients and their parents, which may have caused some bias. The predominant affected side may play an important role in asymmetry of the findings. The number of attacks may additionally contribute to these results. Although the data are not sufficiently accurate and the computing method not particularly appropriate, the total number of attacks should be taken into consideration as an important factor in future studies. Thus, the clinical symptoms of patients may partly explain the asymmetry in our research findings to some extent,[41] but further studies are required for validation.

We observed differences in the ROC results of specific brain regions at distinct frequencies. Previous resting-state studies on PKD predominantly detected abnormalities in brain function within the low-frequency range (<0.1 Hz).[9,10,17] However, different fMRI signal frequencies may have specific physiological relevance.[26] Consistent with previous findings, higher fMRI fluctuations occurred at the slow-4 band (0.027–0.073 Hz) in cortical structures and at the slow-5 band (0.01–0.027 Hz) in subcortical structures.[25] Our current findings suggest that frequency-specific local synchronization potentially contributes to diagnosis of PKD.

Limitations

This study has several limitations. First, the sample size, particularly that of PKD-C patients, was relatively small. In addition, functional findings were possibly confounded by effects of antiepileptic drugs that affect normal brain function. Third, only part of the patients (12/22 PKD-D patients, 6/10 PKD-C patients) took the PRRT2 gene test in the present study. Among these patients who were tested for the PRRT2 gene, 4 out of the 12 PKD-D patients and 2 out of the 6 PKD-C patients were identified with PRRT2 mutations. The frequency of PRRT2 mutations did not differ between the PKD-D and PKD-C groups (chi-square test, $P = 0.46$). It is possible that our small sample size did not provide sufficient statistical power to detect the difference. The absence of difference in the frequency of PRRT2 mutations between the 2 groups is consistent with a previous finding from Huang et al.[8] In that study, the authors found no difference in the frequency of PRRT2 mutations between their PKD-D (15/59 PRRT2 mutation vs 44/59 non-PRRT2 mutation) and PKD-C (2/4 PRRT2 mutation vs 2/4 non-PRRT2 mutation) patients. A recent investigation revealed differences in intrinsic brain activity between PKD with and without PRRT2 mutations.[9] Accordingly, we intend to conduct studies focusing on brain local synchronization between different genotypes of PKD in the near future. Finally, in the present study, we specifically analyzed regional functional measurements and did not take into account the brain connectome as a whole. Further research using multimodal methods may aid in completely defining the underlying mechanisms of the disease.

CONCLUSION

The present study investigated the resting-state local synchronization to determine the neural basis of PKD-D and PKD-C. The present results showed different ReHo between PKD-D and PKD-C groups in the right precuneus, right putamen, and right angular gyrus at the slow-5 frequency band (0.01–0.027 Hz), suggesting frequency-specific abnormal synchronous brain activity in PKD. Our findings collectively provide new insights into the pathophysiology of PKD.

ACKNOWLEDGMENTS

The authors thank the patients, their families, and control subjects. This work would have not been possible without their support.

REFERENCES

1. Demirkiran M, Jankovic J. Paroxysmal dyskinesias: clinical features and classification. *Ann Neurol.* 1995;38:571–579.
2. Bruno MK, Hallett M, Gwinn-Hardy K, et al. Clinical evaluation of idiopathic paroxysmal kinesigenic dyskinesia: new diagnostic criteria. *Neurology.* 2004;63:2280–2287.
3. Frucht SJ. The definition of dystonia: current concepts and controversies. *Mov Disord.* 2013;28:884–888.
4. Cardoso F, Seppi K, Mair KJ, et al. Seminar on choreas. *Lancet Neurol.* 2006;5:589–602.
5. Phukan J, Albanese A, Gasser T, et al. Primary dystonia and dystonia-plus syndromes: clinical characteristics, diagnosis, and pathogenesis. *Lancet Neurol.* 2011;10:1074–1085.
6. Wang JL, Cao L, Li XH, et al. Identification of PRRT2 as the causative gene of paroxysmal kinesigenic dyskinesias. *Brain.* 2011;134:3493–3501.
7. Chen WJ, Lin Y, Xiong ZQ, et al. Exome sequencing identifies truncating mutations in PRRT2 that cause paroxysmal kinesigenic dyskinesia. *Nat Genet.* 2011;43:1252–1255.
8. Huang XJ, Wang T, Wang JL, et al. Paroxysmal kinesigenic dyskinesia: Clinical and genetic analyses of 110 patients. *Neurology.* 2015;85:1546–1553.
9. Luo C, Chen Y, Song W, et al. Altered intrinsic brain activity in patients with paroxysmal kinesigenic dyskinesia by PRRT2 mutation: altered brain activity by PRRT2 mutation. *Neurol Sci.* 2013;34:1925–1931.
10. Zhou B, Chen Q, Zhang Q, et al. Hyperactive putamen in patients with paroxysmal kinesigenic choreoathetosis: a resting-state functional magnetic resonance imaging study. *Mov Disord.* 2010;25:1226–1231.
11. Albanese A, Bhatia K, Bressman SB, et al. Phenomenology and classification of dystonia: a consensus update. *Mov Disord.* 2013;28:863–873.
12. Kim JH, Kim DW, Kim JB, et al. Thalamic involvement in paroxysmal kinesigenic dyskinesia: a combined structural and diffusion tensor MRI analysis. *Hum Brain Mapp.* 2015;36:1429–1441.
13. Joo EY, Hong SB, Tae WS, et al. Perfusion abnormality of the caudate nucleus in patients with paroxysmal kinesigenic choreoathetosis. *Eur J Nucl Med Mol Imaging.* 2005;32:1205–1209.

14. Shirane S, Sasaki M, Kogure D, et al. Increased ictal perfusion of the thalamus in paroxysmal kinesigenic dyskinesia. *J Neurol Neurosurg Psychiatry.* 2001;71:408–410.
15. Zhou B, Chen Q, Gong Q, et al. The thalamic ultrastructural abnormalities in paroxysmal kinesigenic choreoathetosis: a diffusion tensor imaging study. *J Neurol.* 2010;257:405–409.
16. Ko CH, Kong CK, Ngai WT, et al. Ictal (99m)Tc ECD SPECT in paroxysmal kinesigenic choreoathetosis. *Pediatr Neurol.* 2001;24:225–227.
17. Ren J, Lei D, Yang T, et al. Increased interhemispheric resting-state functional connectivity in paroxysmal kinesigenic dyskinesia: a resting-state fMRI study. *J Neurol Sci.* 2015;351:93–98.
18. Poston KL, Eidelberg D. Functional brain networks and abnormal connectivity in the movement disorders. *Neuroimage.* 2012;62: 2261–2270.
19. Holtbernd F, Eidelberg D. Functional brain networks in movement disorders: recent advances. *Curr Opin Neurol.* 2012;25:392–401.
20. Zang Y, Jiang T, Lu Y, et al. Regional homogeneity approach to fMRI data analysis. *Neuroimage.* 2004;22:394–400.
21. Jiang L, Xu T, He Y, et al. Toward neurobiological characterization of functional homogeneity in the human cortex: regional variation, morphological association and functional covariance network organization. *Brain Struct Funct.* 2015;220:2485–2507.
22. Gabrieli JD, Ghosh SS, Whitfield-Gabrieli S. Prediction as a humanitarian and pragmatic contribution from human cognitive neuroscience. *Neuron.* 2015;85:11–26.
23. Jankovic J. Treatment of hyperkinetic movement disorders. *Lancet Neurol.* 2009;8:844–856.
24. Chao-Gan Y, Yu-Feng Z. DPARSF: a MATLAB toolbox for ''pipeline'' data analysis of resting-state fMRI. *Front Syst Neurosci.* 2010;4:13.
25. Zuo XN, Di Martino A, Kelly C, et al. The oscillating brain: complex and reliable. *Neuroimage.* 2010;49:1432–1445.
26. Gohel SR, Biswal BB. Functional integration between brain regions at rest occurs in multiple-frequency bands. *Brain Connect.* 2015;5:23–34.
27. Song X, Zhang Y, Liu Y. Frequency specificity of regional homogeneity in the resting-state human brain. *PLoS One.* 2014;9:e86818.
28. Swets JA. Measuring the accuracy of diagnostic systems. *Science.* 1988;240:1285–1293.
29. Zhu Y, Yu Y, Shinkareva SV, et al. Intrinsic brain activity as a diagnostic biomarker in children with benign epilepsy with centro-temporal spikes. *Hum Brain Mapp.* 2015;36:3878–3889.
30. Jenkinson M, Bannister P, Brady M, et al. Improved optimization for the robust and accurate linear registration and motion correction of brain images. *Neuroimage.* 2002;17:825–841.
31. Mir P, Huang YZ, Gilio F, et al. Abnormal cortical and spinal inhibition in paroxysmal kinesigenic dyskinesia. *Brain.* 2005;128:291–299.
32. Onofrj M, Bonanni L, Pizzi SD, et al. Cortical activation during levitation and tentacular movements of corticobasal syndrome. *Medicine (Baltimore).* 2015;94:e1977.
33. Mehta SH, Morgan JC, Sethi KD. Paroxysmal dyskinesias. *Curr Treat Options Neurol.* 2009;11:170–178.
34. Alexander GE, Crutcher MD. Functional architecture of basal ganglia circuits: neural substrates of parallel processing. *Trends Neurosci.* 1990;13:266–271.
35. Whiteside SP, Port JD, Abramowitz JS. A meta-analysis of functional neuroimaging in obsessive-compulsive disorder. *Psychiatry Res.* 2004;132:69–79.
36. Harris GJ, Pearlson GD, Peyser CE, et al. Putamen volume reduction on magnetic resonance imaging exceeds caudate changes in mild Huntington's disease. *Ann Neurol.* 1992;31:69–75.
37. Vonsattel JP, Myers RH, Stevens TJ, et al. Neuropathological classification of Huntington's disease. *J Neuropathol Exp Neurol.* 1985;44:559–577.
38. Obermann M, Yaldizli O, de Greiff A, et al. Increased basal-ganglia activation performing a non-dystonia-related task in focal dystonia. *Eur J Neurol.* 2008;15:831–838.
39. Margulies DS, Vincent JL, Kelly C, et al. Precuneus shares intrinsic functional architecture in humans and monkeys. *Proc Natl Acad Sci U S A.* 2009;106:20069–20074.
40. Morecraft RJ, Cipolloni PB, Stilwell-Morecraft KS, et al. Cytoarchitecture and cortical connections of the posterior cingulate and adjacent somatosensory fields in the rhesus monkey. *J Comp Neurol.* 2004;469:37–69.
41. Ganos C, Aguirregomozcorta M, Batla A, et al. Psychogenic paroxysmal movement disorders—clinical features and diagnostic clues. *Parkinsonism Relat Disord.* 2014;20:41–46.